Supplementary Information

Mononuclear Copper(II) Complexes with Polypyridyl Ligands: Synthesis, Characterization, DNA Interactions/Cleavages and *in vitro* Cytotoxicity towards Human Cancer Cells

Arabinda Muley[a],† Sadananda Kumbhakar[a],† Rajnikant Raut[b], Shobhit Mathur[a], Indrajit Roy[a], Taruna Saini[b], Ashish Misra[b*], Somnath Maji[a*]

[a]*Department of Chemistry, Indian Institute of Technology, Hyderabad, Kandi, Sangareddy 502284*
Telangana, India

[b]*Department of Biotechnology, Indian Institute of Technology, Hyderabad, Kandi, Sangareddy 502284*
Telangana, India
ashishmisra@bt.iith.ac.in

† These authors contributed equally

Email address: smaji@chy.iith.ac.in (Somnath Maji)

*Corresponding author

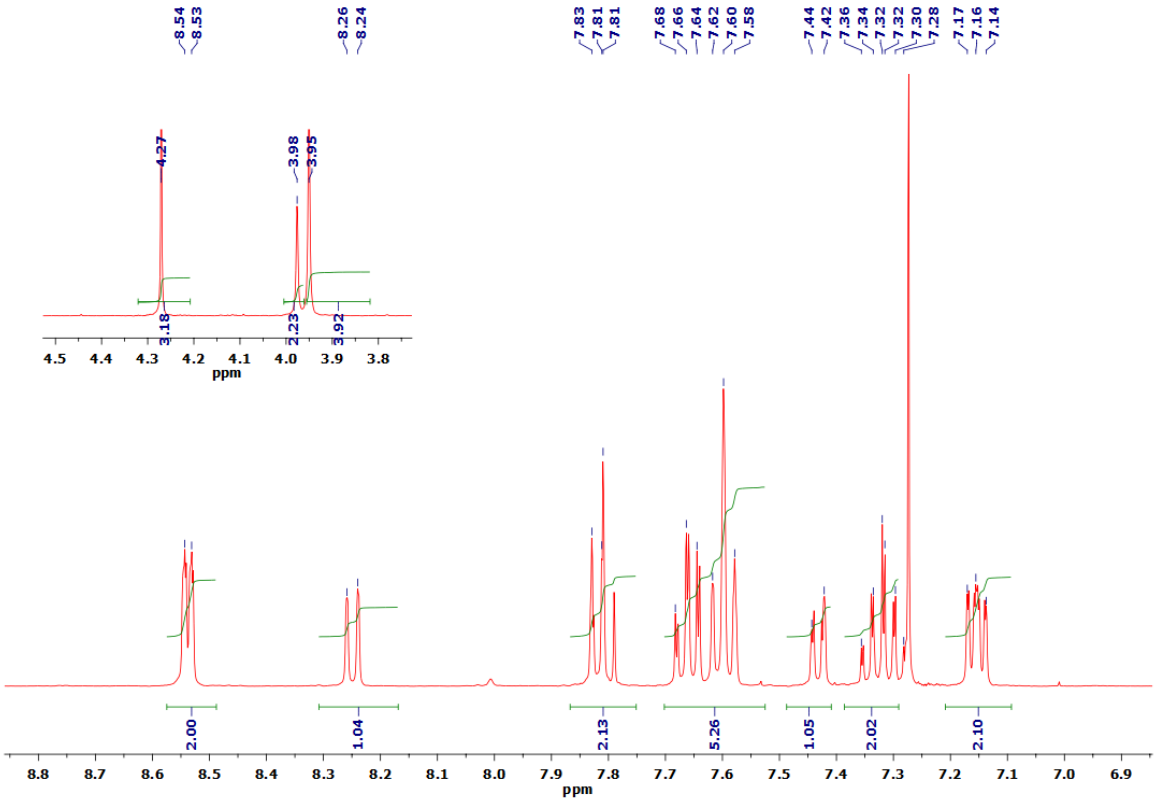

Fig. S1 ^{1}H NMR spectra of **L²** in $CDCl_3$.

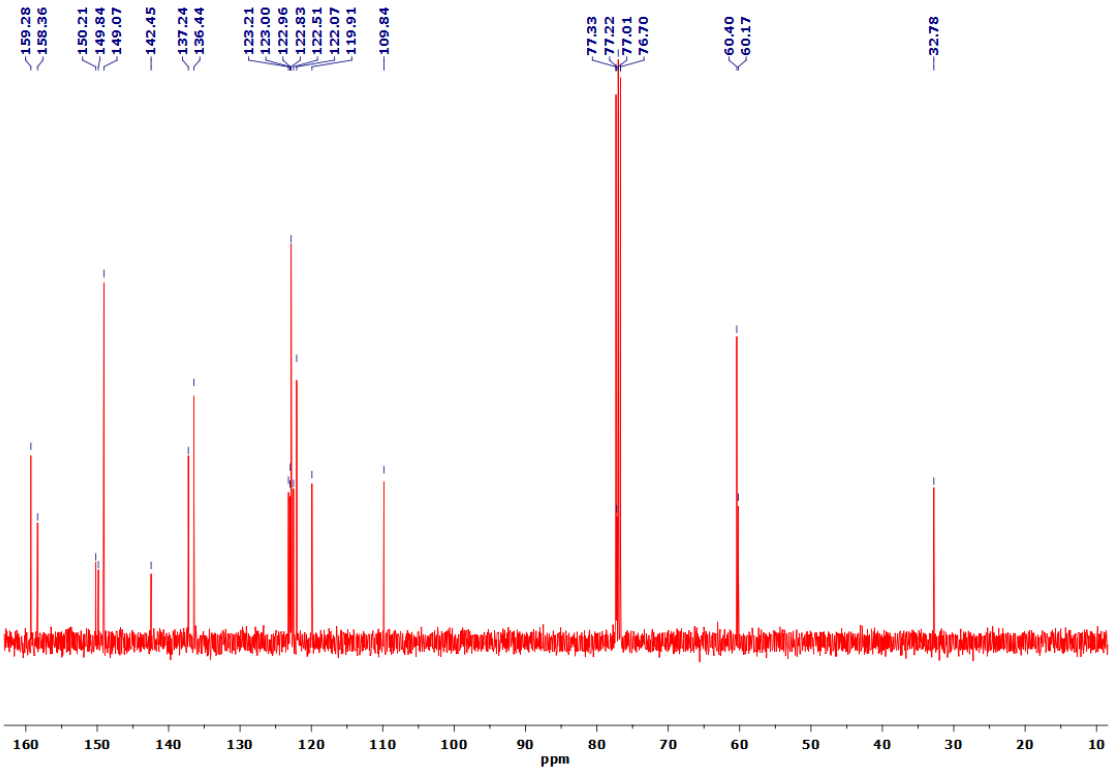

Fig. S2 ^{13}C NMR spectra of **L²** in $CDCl_3$.

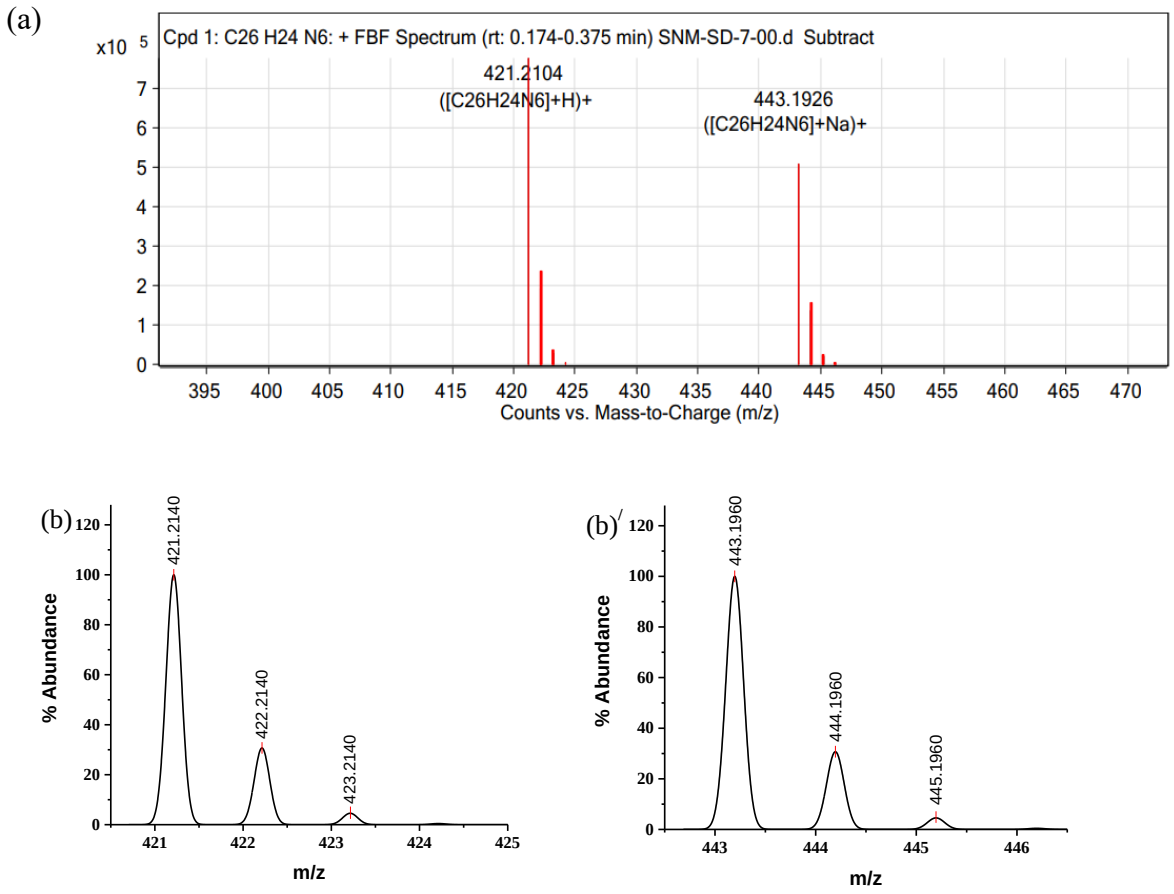

Fig. S3 (a) ESI-MS spectra, **(b)** and **(b)**/ are simulated mass spectra of **L²**.

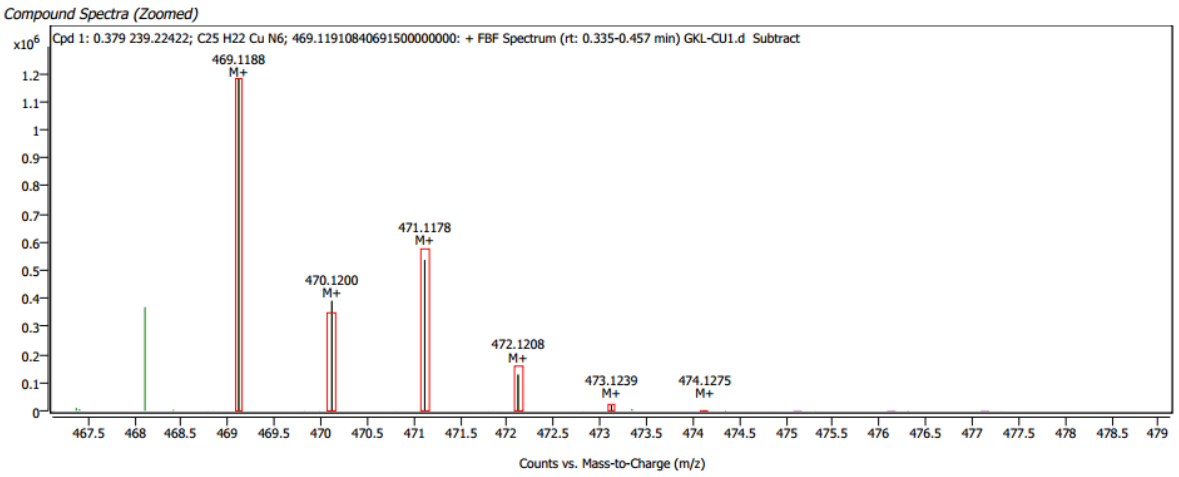

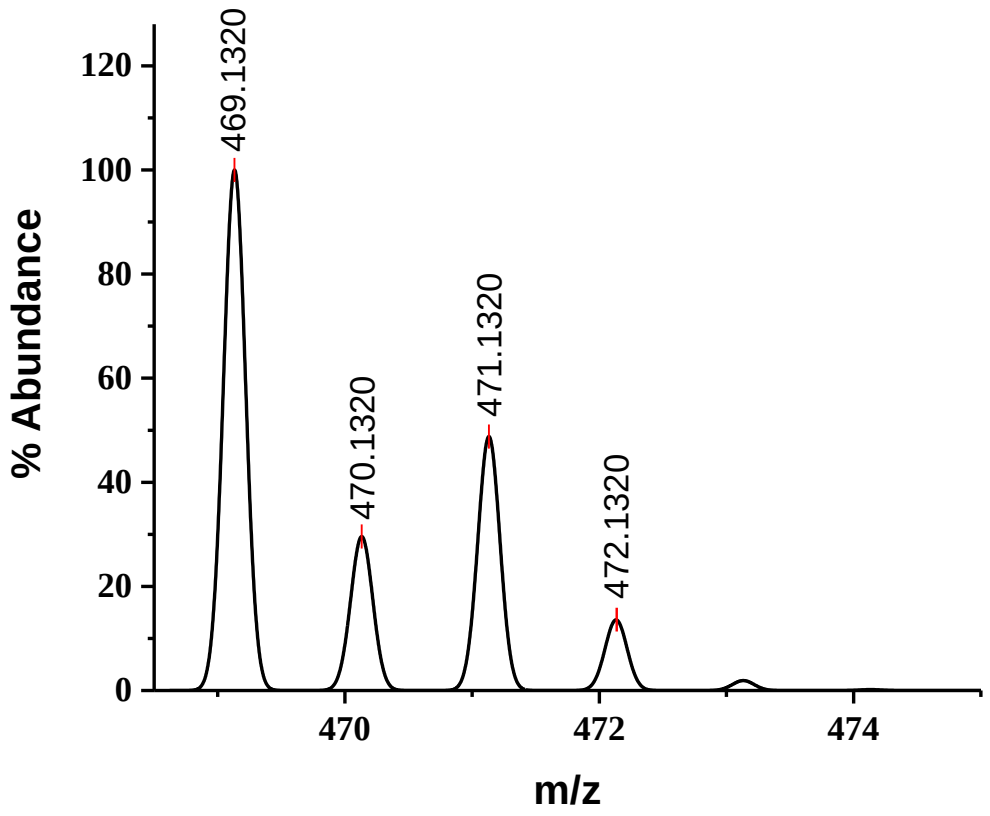

Fig. S4 ESI-MS spectra of [**1**]$(ClO_4)_2$.

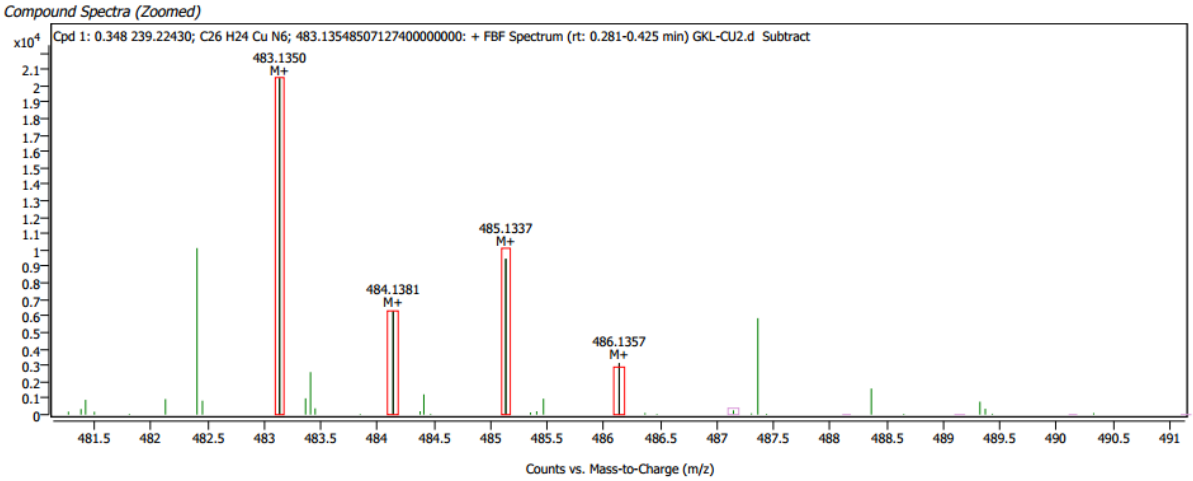

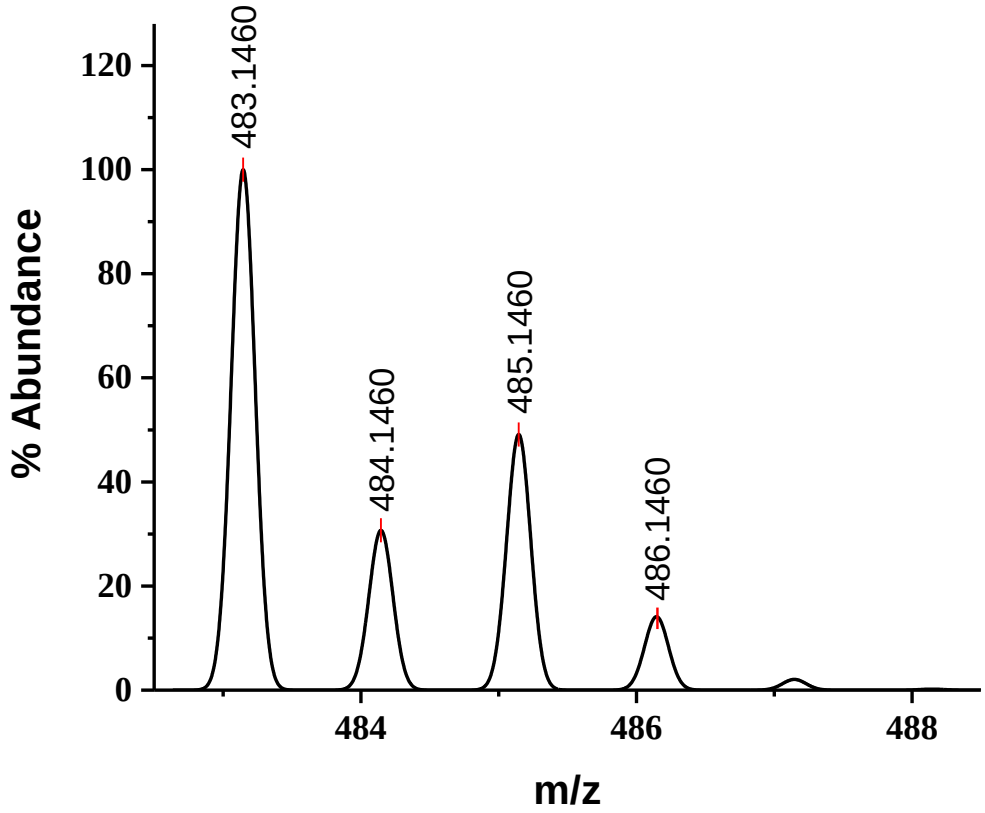

Fig. S5 ESI-MS spectra of [**2**]$(ClO_4)_2$.

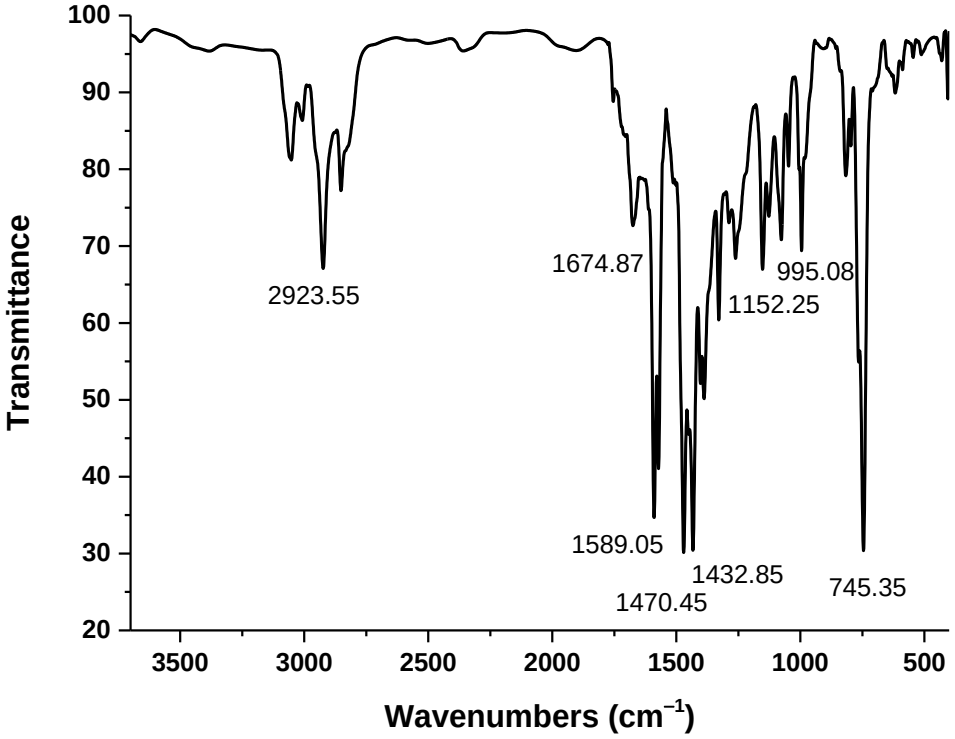

Fig. S6 FT-IR (solid) spectra of **L²**.

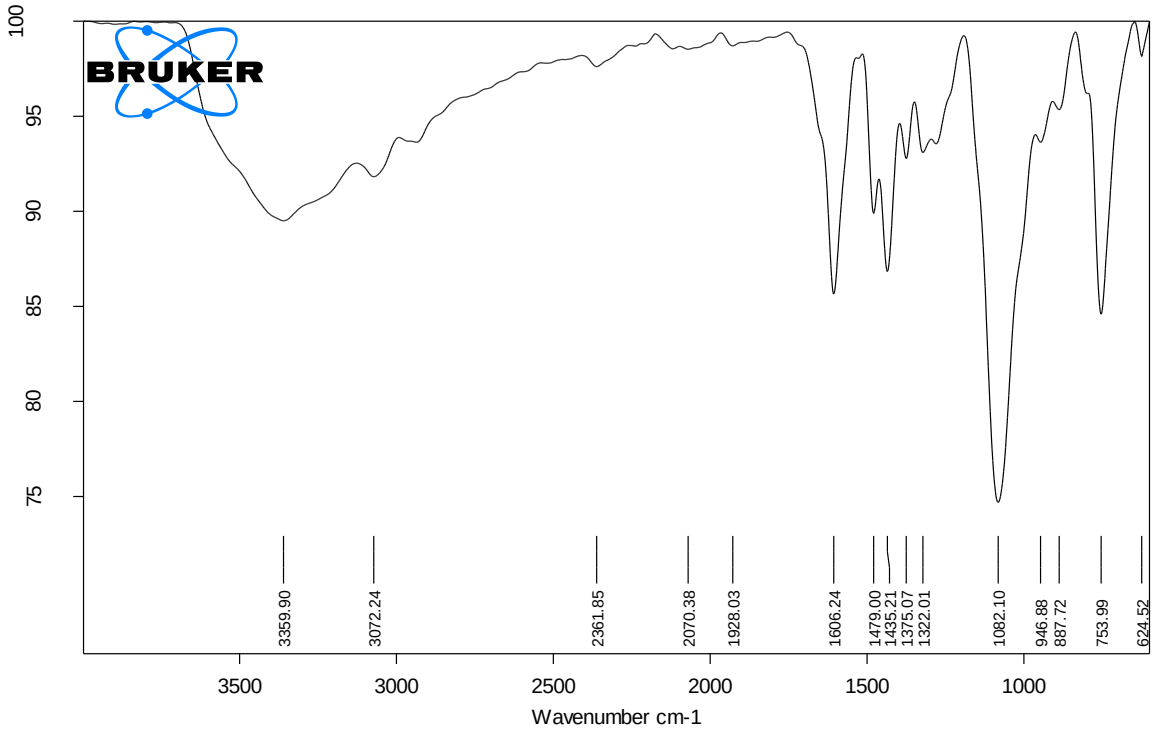

Fig. S7 FT-IR (solid) spectra of [**1**]$(ClO_4)_2$.

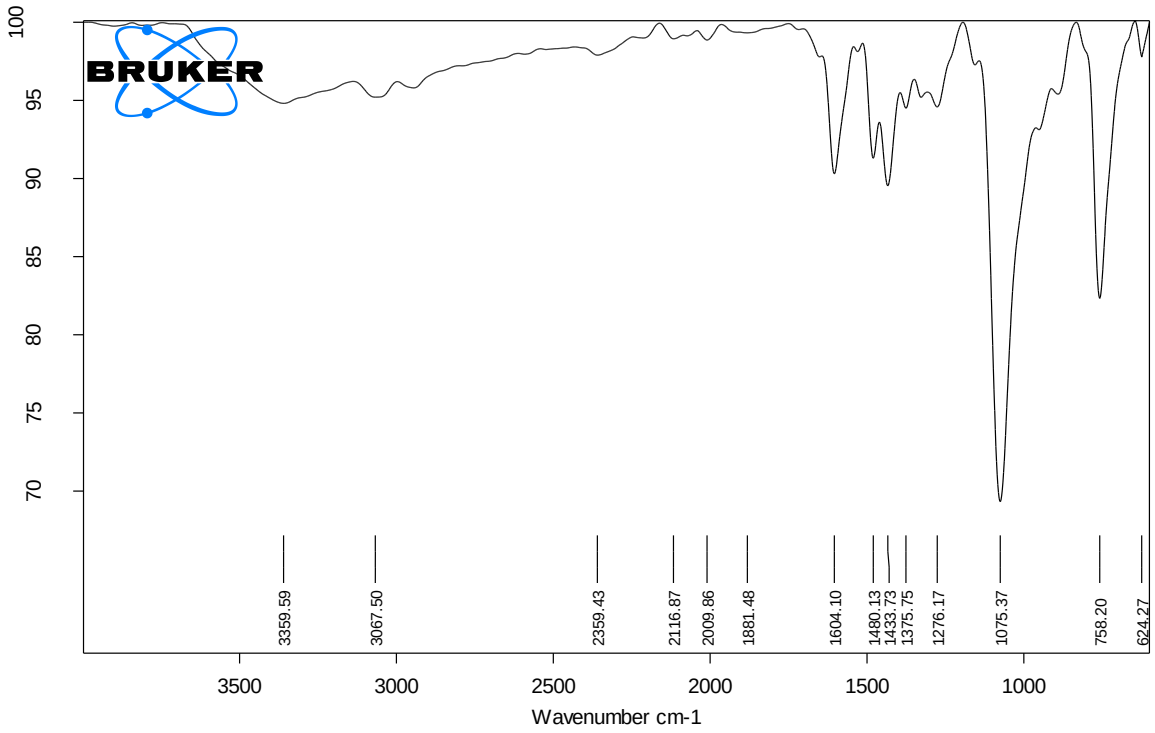

Fig. S8 FT-IR (solid) spectra of [**2**]$(ClO_4)_2$.

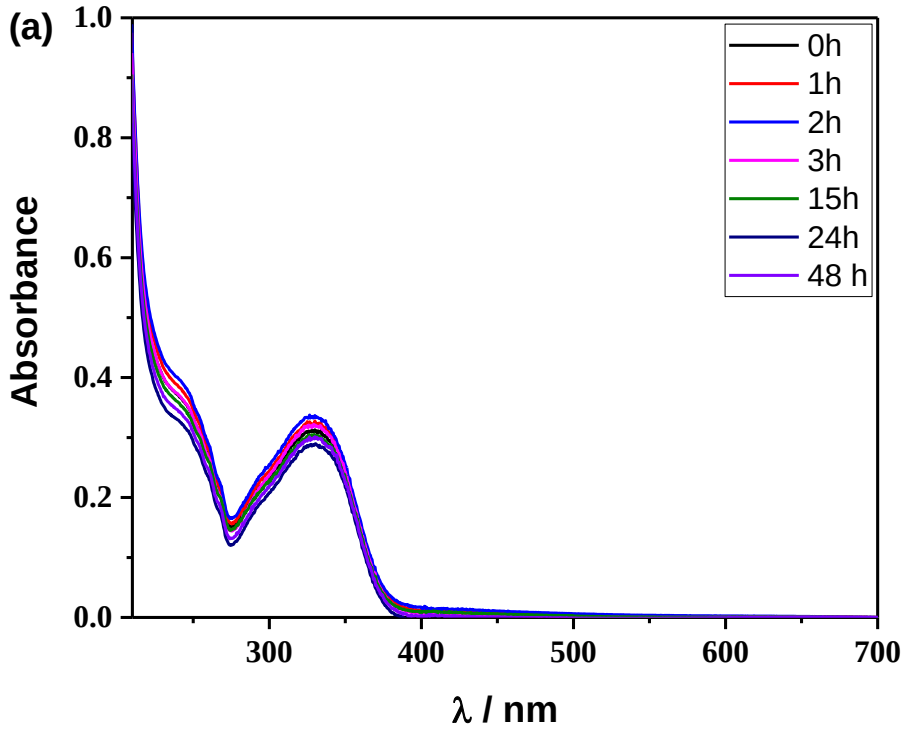

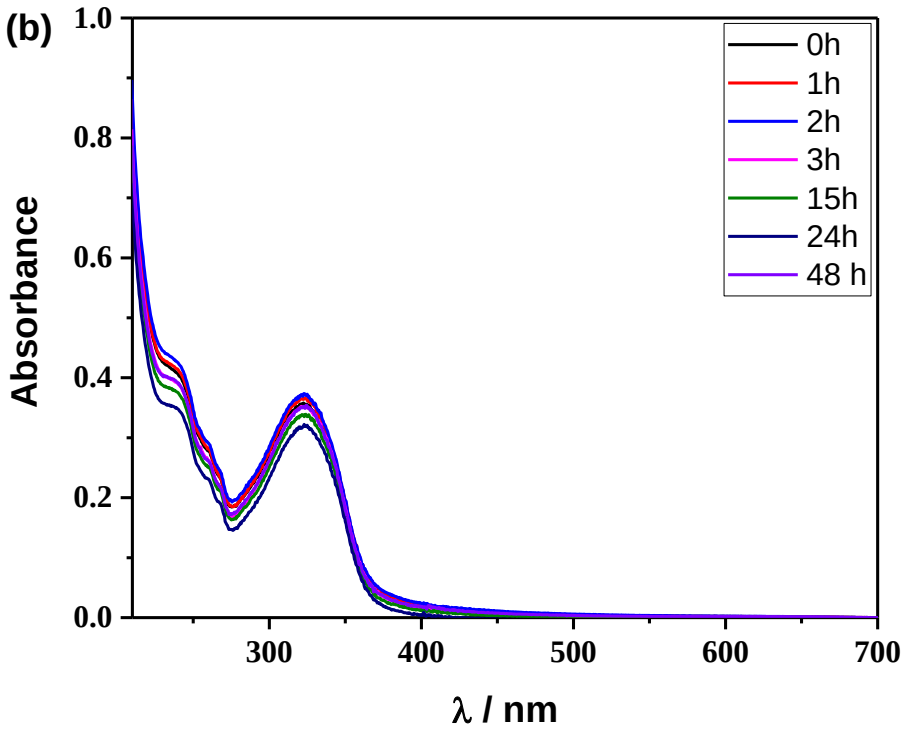

Fig. S9 Stability of (a) [**1**]$(ClO_4)_2$ and (b) [**2**]$(ClO_4)_2$ verified in Tris-HCl buffer solution (pH 7.2) for two days.

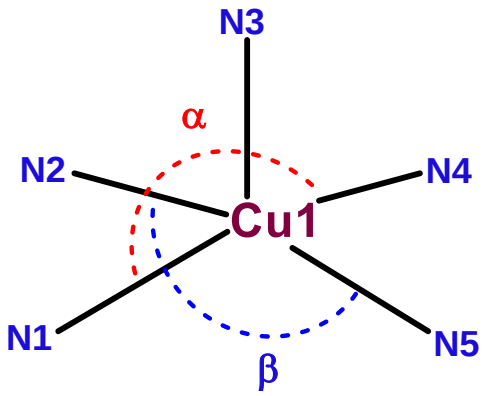

β = 161.54(19), α = 126.30(19)

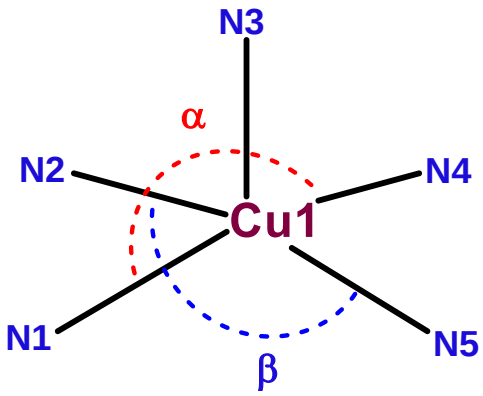

β = 160.58(14), α = 130.25(13)

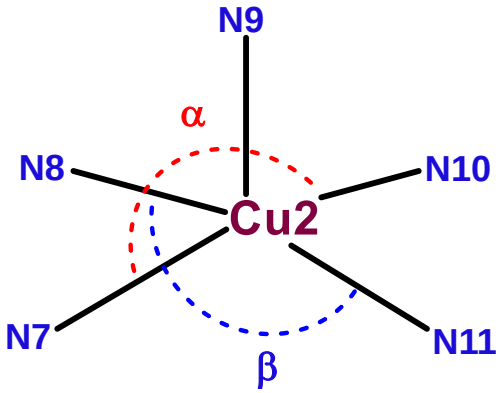

β = 161.3(2), α = 126.83(19)

τ_5 values:

For [**1**]$(ClO_4)_2$
0.58 (Cu1 and Cu2)

For [**2**]$(ClO_4)_2$
0.51

Fig. S10 Schematic representation of [**1**]$(ClO_4)_2$ and [**2**]$(ClO_4)_2$ and respective τ_5 values calculation.

(a)

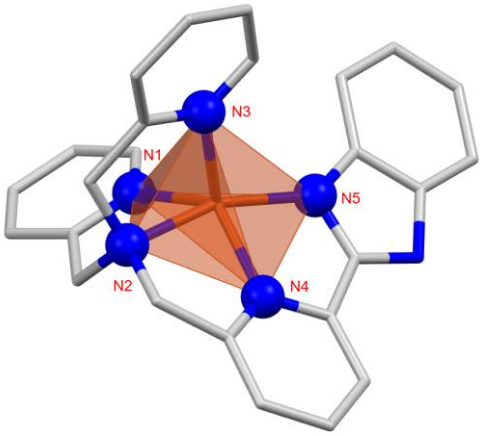

(b)

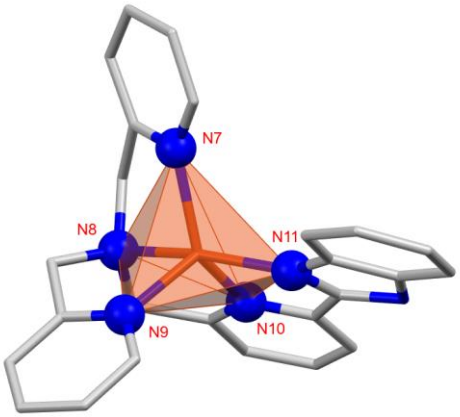

(c)

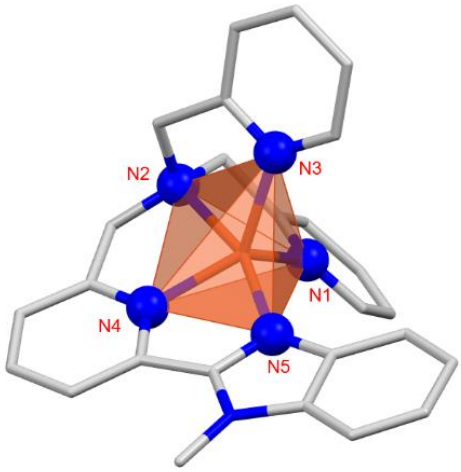

Fig. S11 The polyhedron view of (a) Cu1 center of [**1**]$(ClO_4)_2$ (b) Cu2 center of [**1**]$(ClO_4)_2$ and (c) Cu1 center of [**2**]$(ClO_4)_2$.

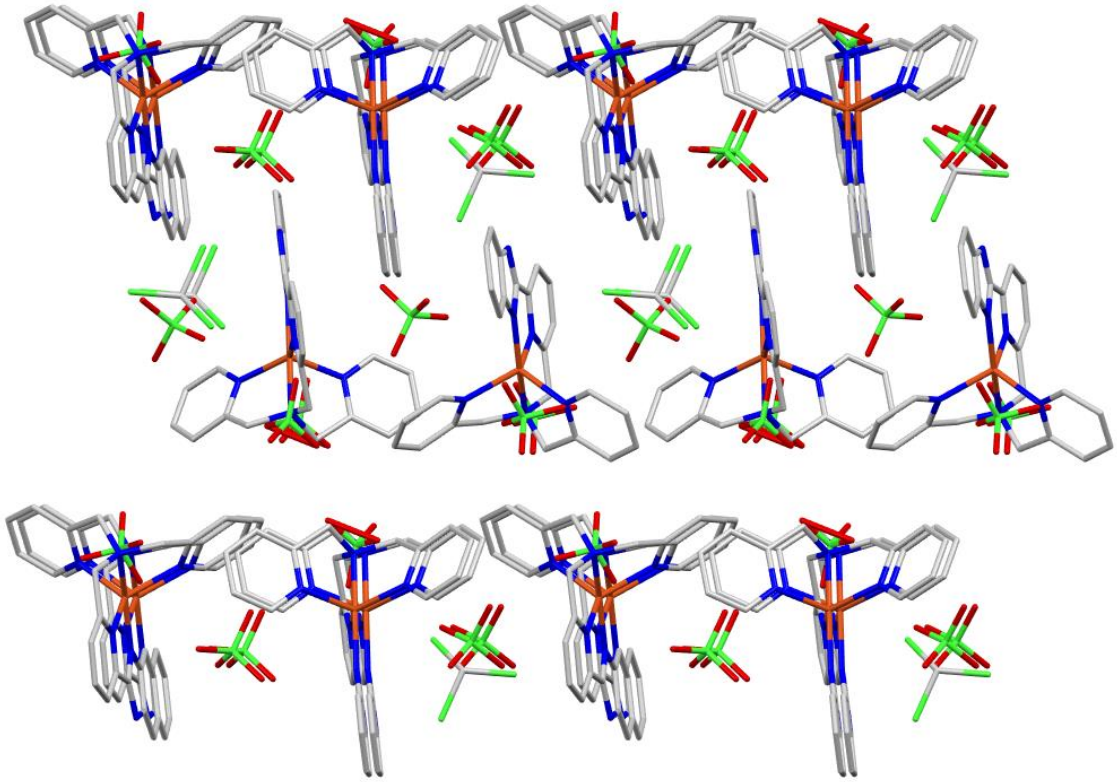

Fig. S12 Crystal packing of [**1**]$(ClO_4)_2$ viewed along *b*-axis.

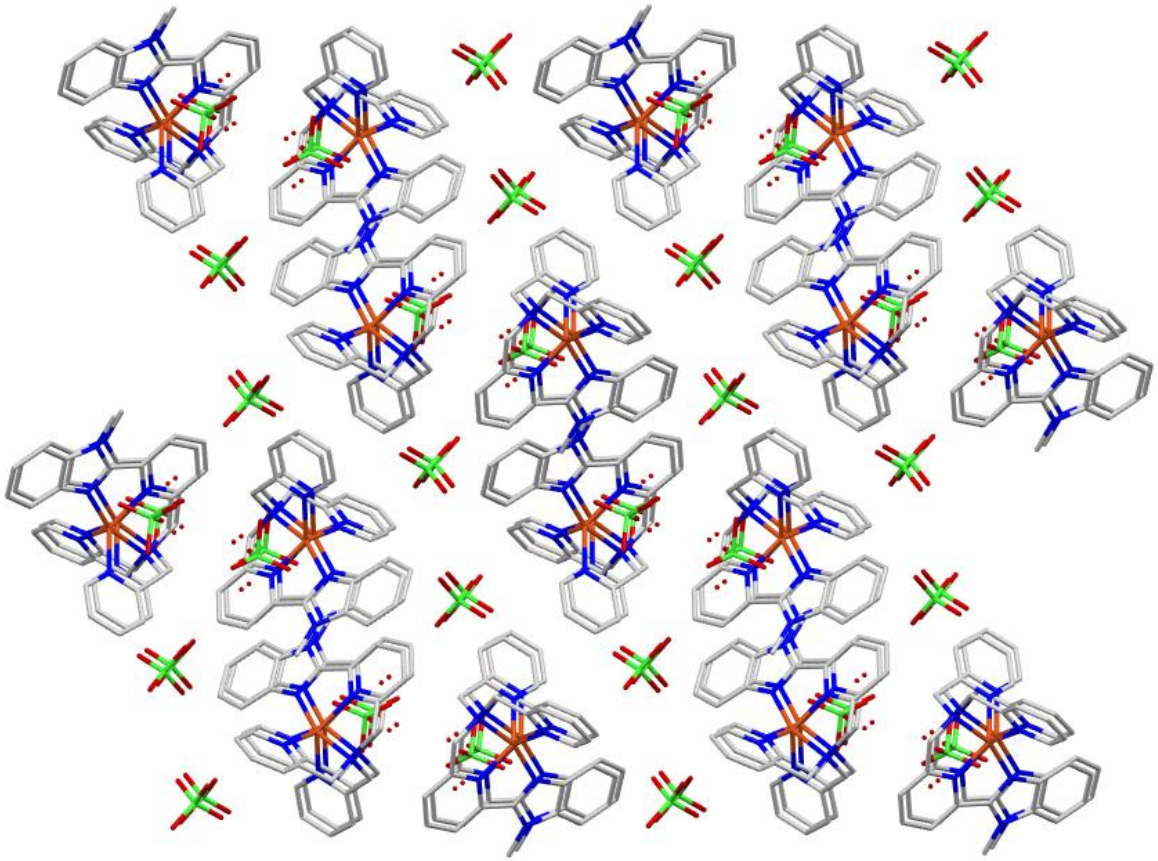

Fig. S13 Crystal packing of [**2**]$(ClO_4)_2$ viewed along *b*-axis.

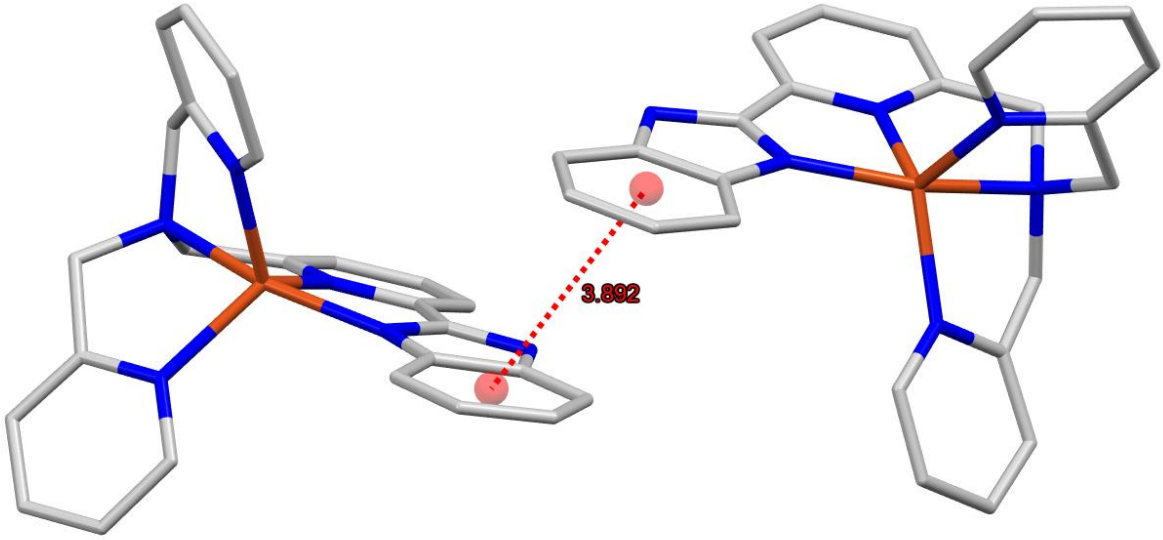

Fig. S14 π–π stacking present in the crystal structures of [**1**]$(ClO_4)_2$.

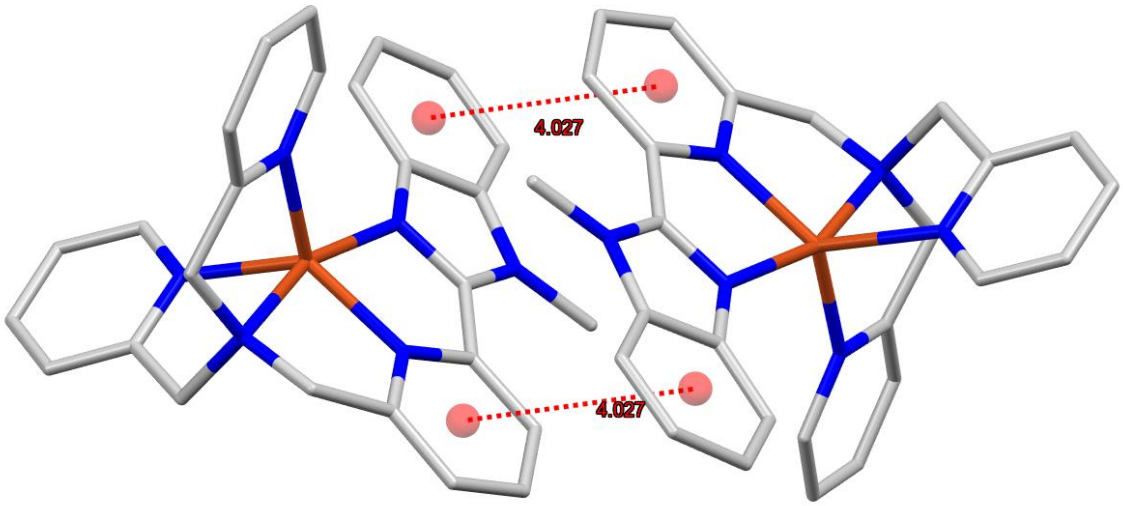

Fig. S15 π–π stacking present in the crystal structures of [**2**]$(ClO_4)_2$.

(a)

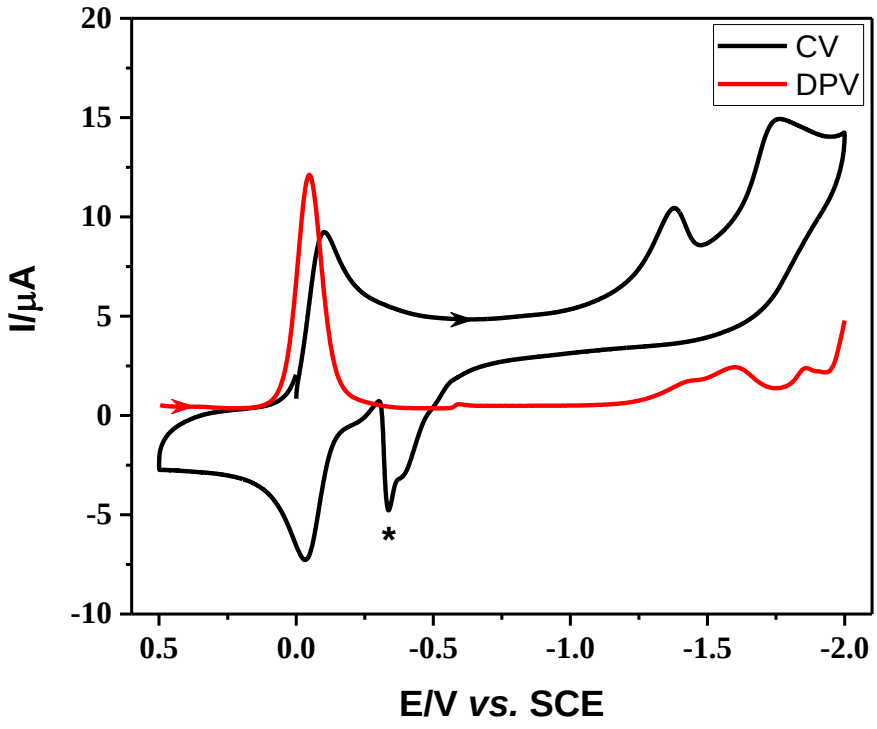

(b)

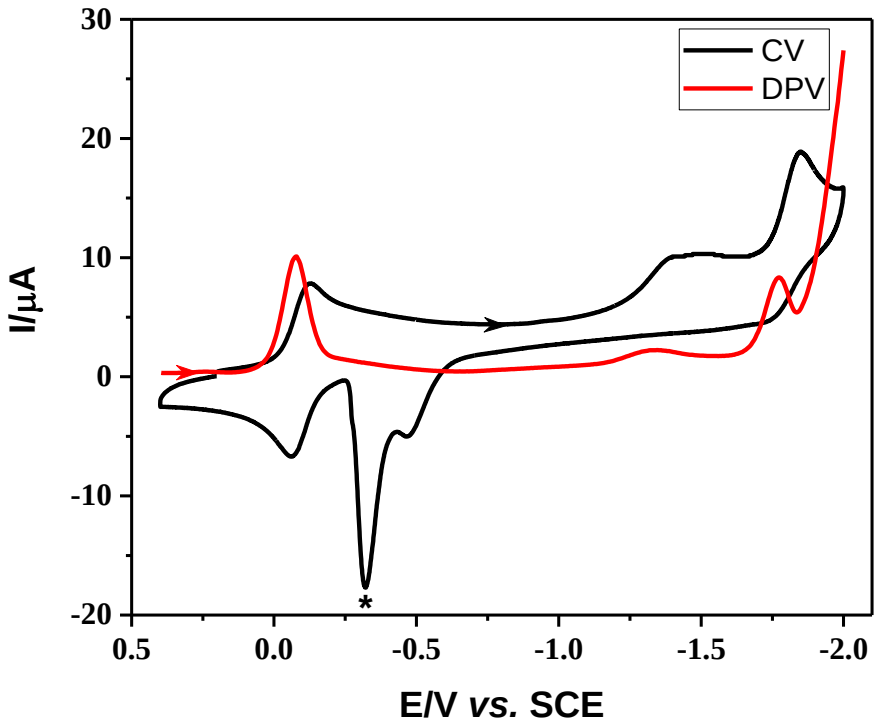

Fig. S16 CV and DPV of (a) [**1**]$(ClO_4)_2$ and (b) [**2**]$(ClO_4)_2$ in acetonitrile using 0.1 M TBAP as supporting electrolyte under argon atmosphere. The peak indicated by * is the deposited copper, for $Cu^0 \rightarrow Cu^I$ oxidation.

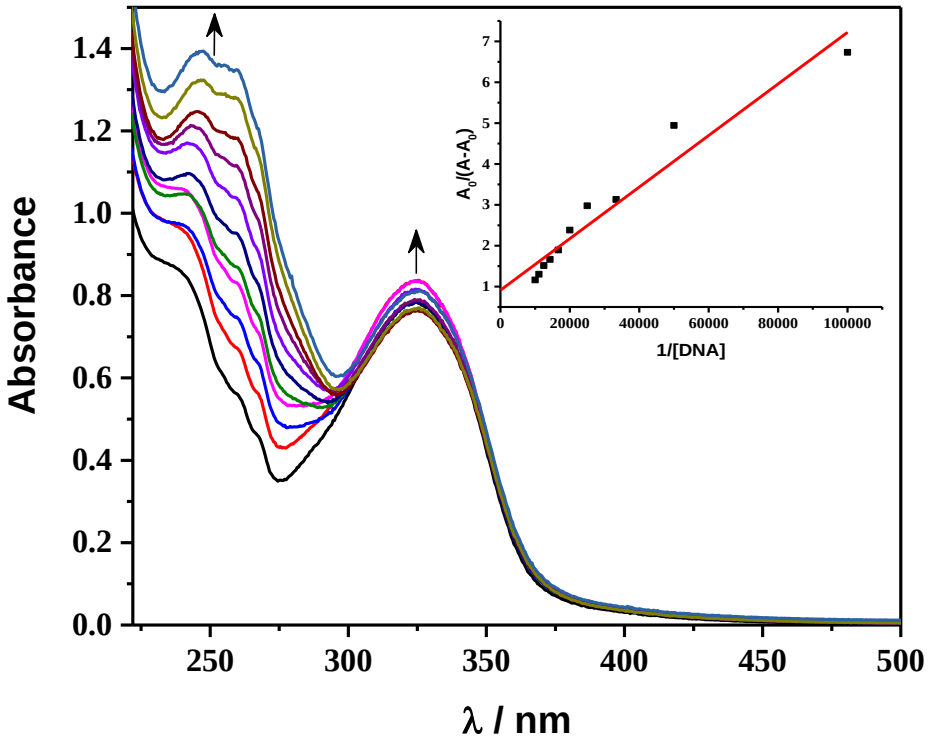

Fig. S17 Absorption spectra of [**2**]$(ClO_4)_2$ (50 μM) in the absence (black) and presence (color) of ss-DNA (10, 20, 30, 40, 50, 60, 70, 80, 90 and 100 μM, respectively) in 5 mM Tris-HCl buffer (pH =7.2). The arrow shows the absorbance changes on increasing DNA concentration. Inset: the plot of $A_0/A–A_0$ versus 1/[DNA] for the calculation of binding constant of complex [**2**]$(ClO_4)_2$.

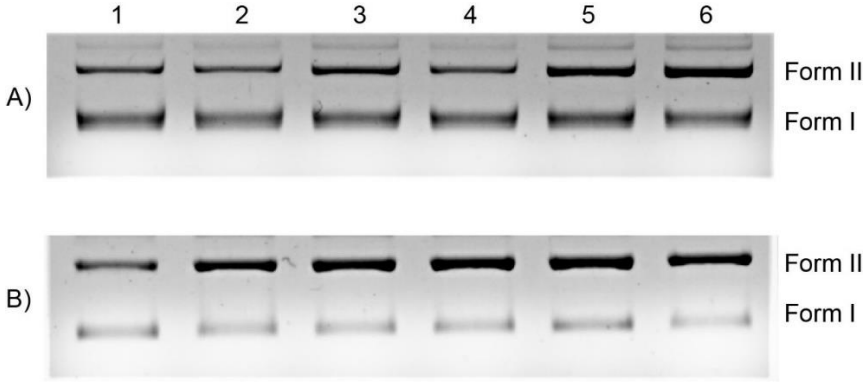

Fig. S18 Agarose gel showing the cleavage of plasmid DNA (pDNA 200 ng/μL) at different concentrations upon incubation at 37 °C for 3 h in 50 mM Tris-HCl buffer (pH 7.2). Lane 1: Control; Lane 2-6 pDNA + complex [**1**]$(ClO_4)_2$ & [**2**]$(ClO_4)_2$ (A-B). The following concentrations range was used for each complex. Complex [**1**]$(ClO_4)_2$: 1μM, 5 μM, 25 μM, 50 μM, 100 μM. Complex [**2**]$(ClO_4)_2$: 5 μM, 10 μM, 25 μM, 50 μM, 100 μM.

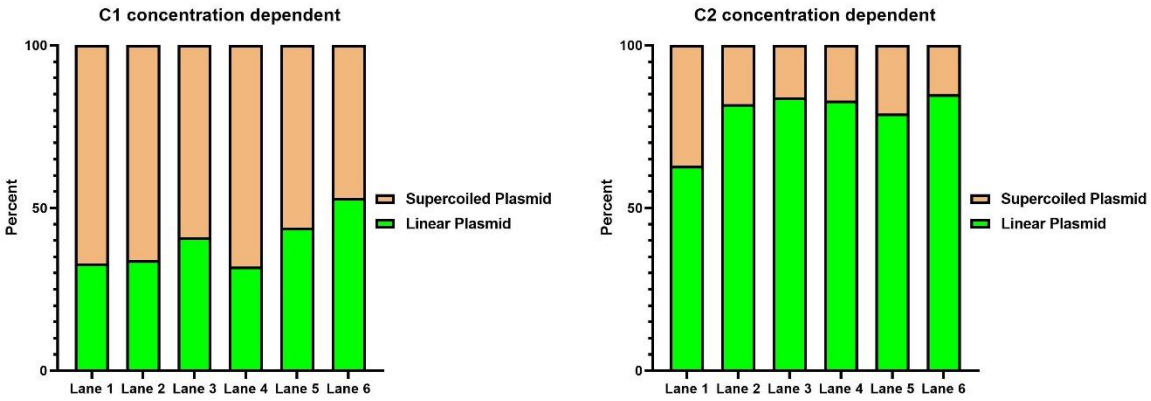

Fig. S19 Histograms representing the coverage of supercoiled and linear DNA in concentration-dependent cleavage assay.

Table S1 Concentration-dependent cleavage assay

[**1**]$(ClO_4)_2$

Sr.No.	Concentrations	Form I (%)	Form II (%)
1	Control	67	33
2	1 μM	66	34
3	5 μM	59	41
4	25 μM	68	32
5	50 μM	56	44
6	100 μM	47	53

[**2**]$(ClO_4)_2$

Sr.No.	Concentrations	Form I (%)	Form II (%)
1	Control	37	63
2	5 μM	18	82
3	10 μM	16	84
4	25 μM	17	83
5	50 μM	21	79
6	100 μM	15	85

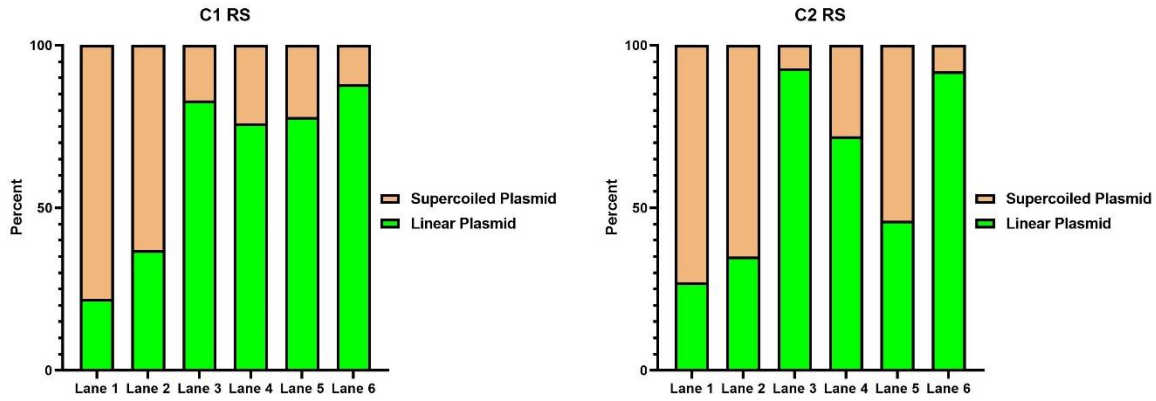

Fig. S20 Histograms representing the coverage of supercoiled and linear DNA in radical scavenging assay.

Table S2 Radical Scavenging assay values

[**1**]$(ClO_4)_2$

Lanes	Form II%	Form I%
Lane 1	22	78
Lane 2	37	63
Lane 3	83	17
Lane 4	76	24
Lane 5	78	22
Lane 6	88	12

[**2**]$(ClO_4)_2$

Lanes	Form II%	Form I%
Lane 1	27	73
Lane 2	35	65
Lane 3	93	7
Lane 4	72	28
Lane 5	46	54
Lane 6	92	8